2014 5th IEEE RAS & EMBS International Conference on
Biomedical Robotics and Biomechatronics (BioRob)
August 12-15, 2014. São Paulo, Brazil

Thermal Supervision During Robotic Laser Microsurgery

Diego Pardo, Loris Fichera, Darwin G. Caldwell and Leonardo S. Mattos

Abstract— **This paper presents a system to supervise tissue temperature during robotic laser surgery. The use of robotic systems for laser surgery provides mechanisms to control the motion of the laser beam and the exposure time of laser radiation, allowing the automatic generation of incisions. This work focuses on the perception side of the problem, developing a technology for the online verification of the thermal state of the tissue during robotic laser microsurgery. Obtaining this information is paramount to enable automatic control of laser incision quality, which is directly related to tissue temperature. A model learned from real data estimates the change in temperature given the exposure time and power of the laser. The model is implemented in the real system and validated during laser incisions on ex-vivo tissue. Results show that the model can reliably estimate the thermal state of the tissue in real-time, and thus is suitable to produce feedback for automatic control of laser incisions.**

I. INTRODUCTION

Lasers have been used in the treatment of otolaryngological head and neck lesions since the early 1970's [1]. Surgeons remove unhealthy tissue from the vocal cords via laser incisions as treatment for laryngeal cancer. The specimen is resected firing the laser along the boundary of the affected tissue. Fig. 1 shows part of the current setup for this type of procedures: The laser beam is directed with one hand, using a joystick-like input device, while the other hand manipulates a forceps to apply traction on the tissue. Surgeons perceive the progress of the surgery through a microscope. In order to obtain the desired incision, the surgeon moves the laser beam manually and decides the amount of time it should be active. Consequently, the resulting incision length and depth depend completely on the surgeon's perception and manipulation skills.

The limitations mentioned above have recently stimulated new research and technological developments in this area, specifically towards the creation of robot-assisted laser microsurgery systems [2],[3],[4]. Robotic technologies can facilitate and greatly improve the precision of laser microsurgeries by eliminating tremor, allowing motion scaling, and by providing enhanced visualization and ergonomic control. Nevertheless, at the present time limited assistive technologies exist to perceive the state of the tissue while it is being exposed to the laser.

Including new technologies to automatically perform incisions also imposes the need to develop systems to supervise this process. This paper presents a technology to supervise the temperature of tissue with the aim of preventing undesired thermal effects during the automatic generation of incisions.

Authors are with the Department of Advanced Robotics, Istituto Italiano di Tecnologia, Via Morego 30, 16163 Genova, Italy. {diego.pardo, loris.fichera, darwin.caldwell, leonardo.mattos}@iit.it

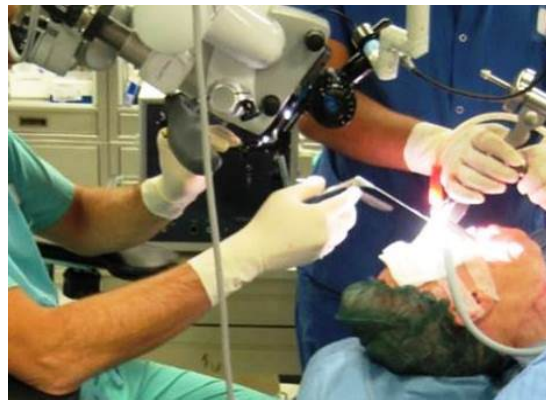

Fig. 1. Setup for laser surgery of the upper aerodigestive tract. The surgeon directs the laser beam operating a joystick-like device with his left hand, while using forceps to put tissue on traction. A microscope is used to obtain a magnified view of the surgical site.

At the present time, no method for the online monitoring of tissue temperature exists that could be readily adopted in laser microsurgery. Traditional approaches require the use of sensing equipment in direct contact with the measurement site [5], thus resulting inappropriate for minimally invasive procedures. Non-invasive techniques based on common medical imaging technologies are being investigated [5]. However, these may require the introduction of substantial changes to the medical protocol, e.g. the use of MRI-compatible equipment. Furthermore, whether these methods account for the dynamic changes in temperature observed in a spatially concentrated area during laser microsurgery is to be verified.

To overcome these drawbacks, here we propose the concept of a system able to monitor temperature without the need for additional sensing devices. The system is based on a model that estimates the temperature on the tissue surface. Such model is derived from data collected during real laser incisions on ex-vivo tissue.

The paper is organized as follows. Section II describes the roll of temperature during the laser incision process. It also reviews the existing models describing the temperature dynamics. Section III describes the technology for the automatic generation of laser incisions. In Section IV a temperature estimation model is derived from real data. Description of the experiments and results are summarized in Sections V and VI, respectively. Finally, conclusions and future work are commented in Section VII.

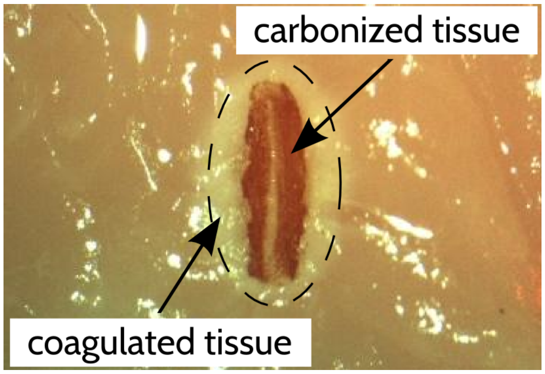

Fig. 2. Effects of CO_2 laser radiation on soft tissue. Dark areas in the surroundings of the incision indicate that temperatures over 100°C have been reached.

II. Tissue Temperature during laser incisions

This section revises the underlying processes occurring when producing laser incisions on soft tissue, motivating the use of a temperature estimation model to supervise thermal effects. Different approaches for modeling are discussed.

A. Laser-Tissue Thermal Interaction

When applying laser light to biological tissue different interactions may occur (e.g., thermal, photochemical, photoablation, photodisruption). The type of laser-tissue interaction depends on the power density ($\frac{W}{cm^2}$) and exposure time (s) [6]. For the case of laser incisions, a *thermal interaction* takes place: tissue molecules are promoted to an excited state due to the absorption of photons, excited molecules collide with partners in the surrounding, such collision leads to the deactivation of the excited molecules and the increasing of the kinetic energy in the partners. Tissue temperature rises microscopically because of the transferred energy from photons to tissue. As tissue is composed mostly of water its molecules start to vaporize at 100°C, resulting in a *thermal decomposition* [6]. In first approximation, cutting tissue can be described as boiling water. Another effect that may occur during a thermal interaction is known as *Carbonization*. Fig. 2 shows carbonized ex-vivo tissue (chicken breast). It occurs when the tissue temperature rises above 100°C [6]. Carbonization indicates the tissue was burned during the cutting process. It is a non-intentional effect that decreases the quality of surgical procedures, resulting in non ideal cicatrization and the formation of scar tissue. Surgeons keep the laser exposure long enough for cutting, but short enough to avoid carbonization. The onset of carbonization is determined by the temperature at the incision and how it spreads out in space as times goes on [7].

B. Modeling tissue temperature dynamics

The temporal change on temperature at certain point of the tissue, given a laser input, can be modeled using the *Heat Diffusion Equation* [6], [7],

$$\frac{\partial T}{\partial t} = \frac{\kappa}{\rho C_p}\nabla^2 T + \frac{1}{\rho C_p}u, \qquad (1)$$

where $T\,(^\circ C)$ denotes the temperature at the point of interest, $\kappa\left(\frac{W}{m^\circ C}\right)$ is the tissue thermal conductivity, $\rho\left(\frac{kg}{m^3}\right)$ and $C_p\left(\frac{J}{kg^\circ C}\right)$ represent the tissue density and specific heat capacity. The input of the system $u\left(\frac{W}{cm^3}\right)$ is the energy absorbed per unit of volume and time, which depends on the location of the point of interest and varies with time. The nominal value of the input depends on the absorption coefficient, $\mu_a\left(\frac{1}{m}\right)$, of the tissue to the corresponding wavelength of the laser light. Although the analytical model unequivocally describes the elements involved in the change of temperature, the main disadvantage of it relies on the temporal and spatial dependencies of u. Additionally, most of the times this model is numerically evaluated, as its solution implies assumptions on the boundary conditions [6]. Thus, the analytical model is not suitable to be used for the online estimation of the temperature of the tissue during laser surgery.

Numerical simulation of this phenomenon have also been developed. In [12] [13] and [14] different types of simulations are presented to reproduce the change on tissue temperature during single point laser incidence. Although using different simulation methods, these models were used to supervise deep locations in the tissue during low power radiation, i.e., not during incisions. In [8] we presented a simulation of the temperature dynamics on soft tissue during *single point incision*. The purpose of the simulation was to generate data to learn a model of the relationship between input variables similar to those used during laser surgery (i.e., laser power and activation time) with the resulted change in temperature. It was shown that this phenomenon can be modeled using machine learning techniques.

The motion of the laser beam includes an important challenge to the objective of modeling the thermal effects. The function describing the input u in (1) should include this behavior. None of the modeling approaches presented above consider the case of a moving laser beam.

In this work we go further, estimating the temporal change of the temperature at the surroundings of a laser incision, i.e., taking into account the motion of the laser. Such model is derived from experimental data captured during real laser incisions on ex-vivo tissue (chicken breast). The model is suitable to produce online estimation of temperature synchronized with the automatic generation of incisions.

III. Automatic generation of laser incisions

The motion of the laser beam is controlled using a motorized micromanipulator developed in our laboratory [10]. The activation time of the laser is precisely controlled with a piezo controller system (PI E-517). Fig. 3 depicts the concept of this technology.

Automatic incisions are then created moving the laser beam along a line of length (l) during certain exposure time (t_{exp}). The motion of the laser scans the complete line at a configurable velocity and oscillatory frequency (w). Therefore, the number of times the laser scans the incision is given by $\eta = t_{exp}/w$. The period of time the tissue

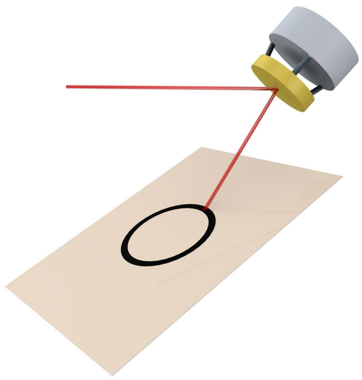

Fig. 3. Robotic laser micromanipulation system. The beam is deflected on the target by a 2-DOF steering mirror, which can be controlled to produce automatic laser trajectories.

is exposed to the laser is uniformly distributed along the incision line. The system can generate any trajectory encoded as a sequence of points. The width of the incision is variable and it is mostly determined by the laser exposure time, nevertheless it can be roughly approximated by the size of the projection of the laser beam on the target, i.e., the laser spot. In the system used in this research, maximum power density is obtained when the laser spot is focused with a radius of $r_s = 250\mu$m.

The distribution of the energy in the laser beam is Gaussian. This beam profile is known as TM_{00} [9] where most of the energy is concentrated in the center of the incidence point. Consequently, the spatial profile of the heat transferred to the tissue is also Gaussian.

For single point laser exposure, the change on temperature on the tissue surface may be modeled as a temporal change of the parameters of a single Gaussian. Contrarily, the motion of the laser beam imposes the use of a more explicit model. In the following section we analyze the temporal change on temperature on the tissue surface from real data, from which the structure of the model is then derived.

IV. Temperature Analysis

Incisions on ex-vivo (chicken breast) tissue were generated using the robotized system. Temperature of the surface was collected using a thermal camera providing a stream of images at a certain resolution. Each image is organized as a matrix of values representing the temperature of the corresponding point in the scene.

Let $T \in R^{m \times n}$ be a two-dimensional matrix representing the values of temperature of a continuous rectangular plane S of known length (Y) and width (X). The temperature of any point $x, y \in S$ will be given by the (i, j)-element of the matrix, following the quantizations,

$$i = \left\lceil \frac{y}{\Delta_y} \right\rceil \quad , \quad j = \left\lceil \frac{x}{\Delta_x} \right\rceil \tag{2}$$

where $\Delta_y = Y/m$, $\Delta_x = X/n$, and the $\lceil \cdot \rceil$ notation expresses the ceil function.

During laser exposure, temperature values of the surface change with time, i.e.,

$$T(S) = f(x, y, t). \tag{3}$$

The camera provides images at a constant rate ($\Delta t = 0.01s$), thus data is available at certain times instances, i.e., $t = k\Delta t$.

Examples of the temperature profile for different times of the process $T(S, k)$ are shown in the first row of Fig. 4. With the aim of reducing the problem complexity, symmetry is assumed in the y axis, and the temperature along the x axis is shown. It can be observed that the Gaussian distribution of the energy in the laser beam is present in the shape of the resulted temperature profile, nevertheless, as the beam moves along the incision, the temperature profile does not show any particular pattern as it grows in time.

On the other hand, the temporal increment of the temperature $\Delta T(k) = T(S, k+1) - T(S, k)$ can be described as a set of of Gaussian functions that moves along the incision line. Second row of Fig. 4 shows the temperature increments for the corresponding exposure time. Initial observations suggest that the positive part of ΔT is always described by a single Gaussian, while the negative part shows diverse conformations. The positive part corresponds to the effect of the laser incidence plus the contribution of underlying heated tissue. Thus, the center of this Gaussian is expected to move together with the laser beam along the incision. The negative part of this function corresponds to the *cooling down* process, which in (1) is denoted by the Laplace operator ($\nabla^2(\cdot)$). This second order term confirms the observation that the shape of the negative part should contain higher order differences of $T(S, k)$.

We hypothesize that the function describing the temperature of the surface at each frame of the process can be approximated as a sum of Gaussian functions,

$$T(S, k) = \sum_{i=1}^{p} \exp(x, y, a_i, \sigma_i, \mu_i) \tag{4}$$

where p is the total number of Gaussian functions and a_i, μ_i and σ_i the corresponding amplitude mean and covariance. Nonlinear least square fitting regression [11] can be applied to fit (4) to the experimental data.

V. Experiments

Incisions on ex-vivo tissue were produced using a commercial surgical laser - Zeiss Opmilas CO_2 25 : wavelength 10.6 μm, TEM_{00} beam profile with Continuous Wave (CW) and 2—25W power range. The motion of the laser beam is controlled by a motorized micromanipulator. Fig 5 shows the system components.

Data is provided by a digital thermal imaging camera (FLIR A655, measurement range: -40 to 250 °C) equipped with a filter for CO_2 emissions. The output from this camera is a stream of video images with a resolution of 640×480 pixels at a frame rate of 100Hz. The region of interest was defined to be $m = 40 \times n = 60$ pixels, capturing the

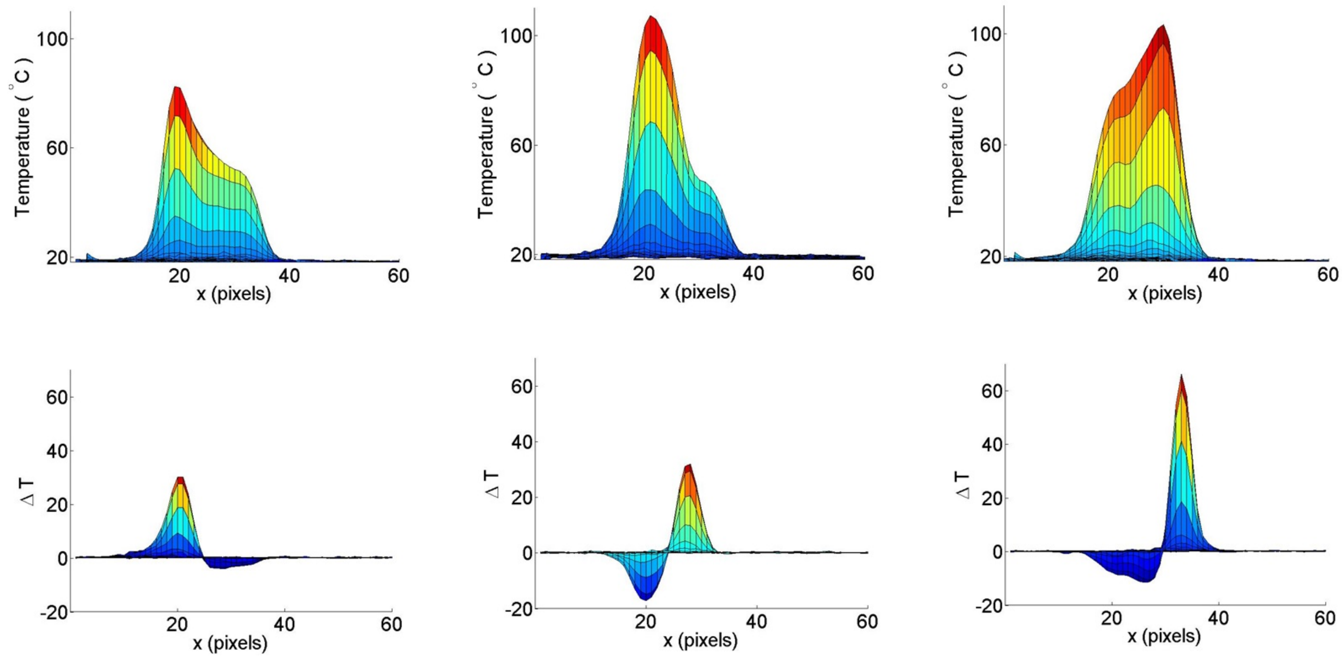

Fig. 4. First row: Tissue temperature profile during computer controlled incision ($l = 0.3mm, w = 10Hz$). Although the Gaussian distribution of the energy in the laser beam is present, the profile does not show any particular pattern as it grows in time. Second row: Temporal change on temperature $\Delta T = T(S, k+1) - T(S, k-1)$

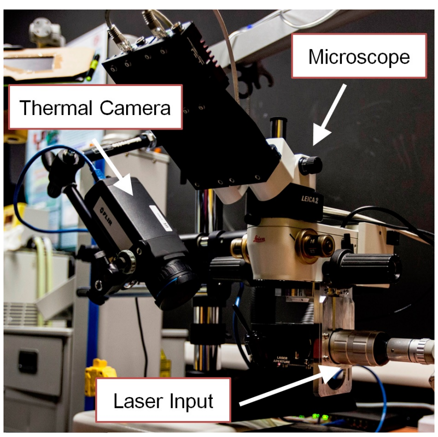

Fig. 5. Experimental setup: Thermal camera, microscope, and laser system.

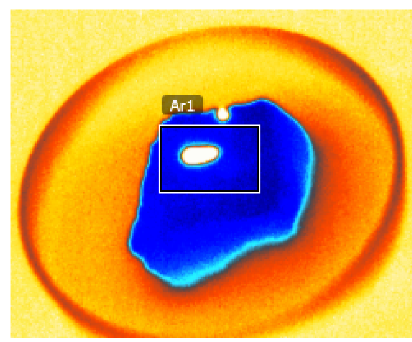

Fig. 6. Thermal image of the tissue target captured during incision process.

region where the incision takes place. This field was selected observing the heat propagation. Distance from the camera to the tissue was maintained constant.

An incision similar to those used during microsurgery is chosen to be modeled. Incision length ($l = 4.6mm/25pixels$) and scanning frequency ($w = 10Hz$) are kept constant. Fig. 6 shows a thermal image of the ex-vivo chicken tissue during the generation of the incision. The area of interest (S) is also shown. Laser power ($P = 3$W), and exposure mode (Continuous Wave) were also configured. Total exposure time is set to $t_{exp} = 1.0s$.

VI. Results

The x-axis is aligned with the incision line and the spatial distribution of the temperature is assumed to be symmetric with respect to the y-axis. Here we compare the quality of the model for different values of p. Based on the knowledge provided by (1), we may hypothesize that the number of Gaussians required for the model is $p = 4$. Nevertheless here we compare the models for different values of p.

For the simplified case of one-dimensional distribution of temperature, the temperature on the incision line $T_k(x)$ is defined by the function

$$T_k(x) \approx \sum_{i=1}^{p} \exp(x, \mu_i, \sigma_i) \tag{5}$$

Each experiment is composed by 100 data sets ($t_{exp} = 1.0s, \Delta t = 0.01s$). The number of input-output pairs per data set is given by the width (in pixels) of the area of interest. Thus, the model is composed by a total of 100 regressions, each one is obtained using $m = 60$ data pairs $\{x_j, T_j\}_{j=1}^{m}$. Fig. 8 shows three examples of function approximated.

TABLE I
REGRESSION RESULTS ANALYSIS: MEAN SQUARE ERROR FOR $n = 100$ REGRESSIONS.

p	MSE_{max}	MSE_{min}	mean	median	Q3 - Q1
3	17.5740	0.2417	3.4297	2.9353	2.0371
4	6.8735	0.2172	2.3121	1.9963	1.7247
5	4.6750	0.2373	1.8510	1.6354	1.3536

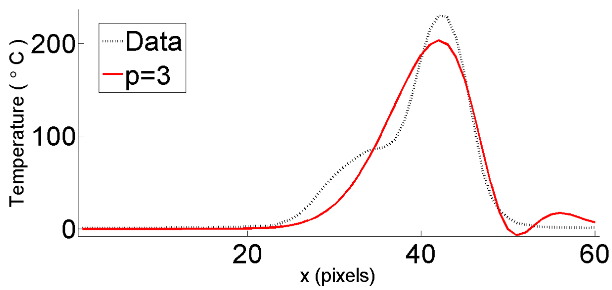

Fig. 7. Regression result (p=3). Real temperature is also shown.

A. Modeling error

The output of the regression at each time step is a vector of parameters (amplitudes, means and standard deviation), $\theta_k = [a_k, \mu_k, \sigma_k]$, where $a, \mu, \sigma \in \mathbb{R}^p$. Each data set generates an approximation error, i.e., it is variable along the experiment. The mean square error (MSE) is analyzed to compare the quality of the model for different values of $p = 3, 4, 5$.

Table I summarizes the information about the variability of the regression error along the experiment, including maximum, minimum, mean, median and interquartile range. It can be seen that the model fits better when using more Gaussians: $p = 4$ performs better than $p = 3$, while not significant improvements can be observed by increasing the number of basis functions to $p = 5$. Fig. 7 shows the temperature estimation when modeling with few Gaussian basis functions. On the other hand, Fig. 8 shows three examples of regressions with $p = 4$. Different forms of temperature profile are shown.

B. Model Validation

Based on the analysis presented above, a model using $p = 4$ is selected to estimate the temperature dynamics during laser exposure. A total of 12 parameters for each time step are used for prediction.

In order to validate the model, a new experiment is performed and thermal data is captured while the model estimates the temperature profile. Validation error is computed pixel-wise during $t_{exp} = 1s$. Fig. 9 shows the real temperature profile for the validation experiment and the resulted temperature estimation (for the same time steps used in Fig 8). It can be observed that the new experiment slightly varies with respect to the learning data set. This causes a relatively high pixel-wise error, as presented in Table II.

Nevertheless, the range and distribution of the temperature is effectively estimated at each time step. In order to illustrate

TABLE II
VALIDATION RESULTS ANALYSIS: MEAN SQUARE ERROR FOR $n = 100$.

p	MSE_{max}	MSE_{min}	mean	median	Q3 - Q1
4	19.27	4.4438	12.52	13.4160	10.3432

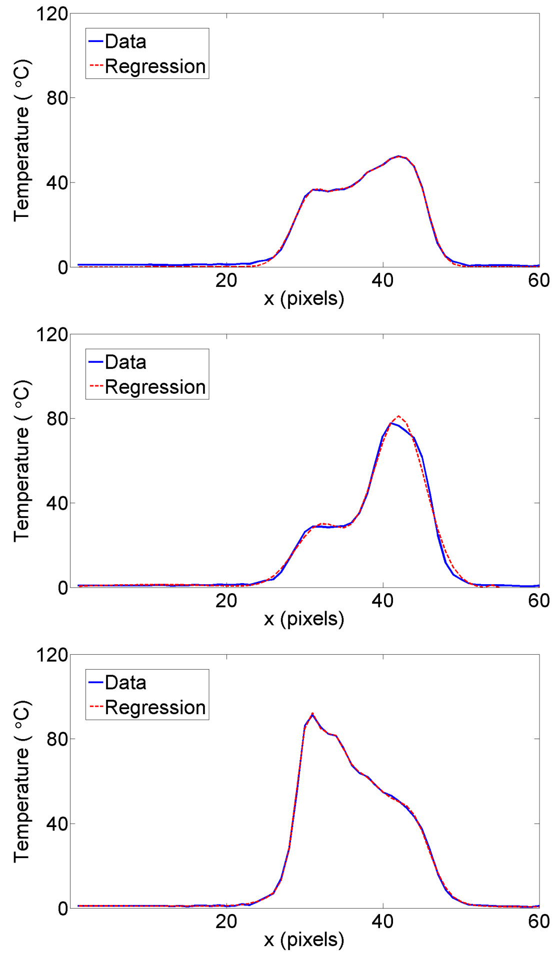

Fig. 8. Temperature profile at different stages of the incision. Continuous line (blue) shows data collected from experiments, dash line (red) shows the result of the regression $p = 4$.

this, a comparison between the maximum value at each time step is shown in Fig. 10. It can be observed that the model captures the dynamics of the temperature change. The shape of the temperature profile is compared by computing the area under the curve at each time step, also shown in Fig. 10. It can be observed that the model is able to effectively estimate the thermal state of the tissue surface.

VII. CONCLUSIONS AND FUTURE WORK

A model able to reliably estimate tissue temperature variations during laser incisions on soft tissue was developed. The model is extracted from real thermal data collected during automatic laser incisions on ex-vivo tissue (chicken breast). Further efforts will be directed towards the creation of a more realistic model that captures the temperature dynamics in living tissue. Although some heat transfer mechanisms typical

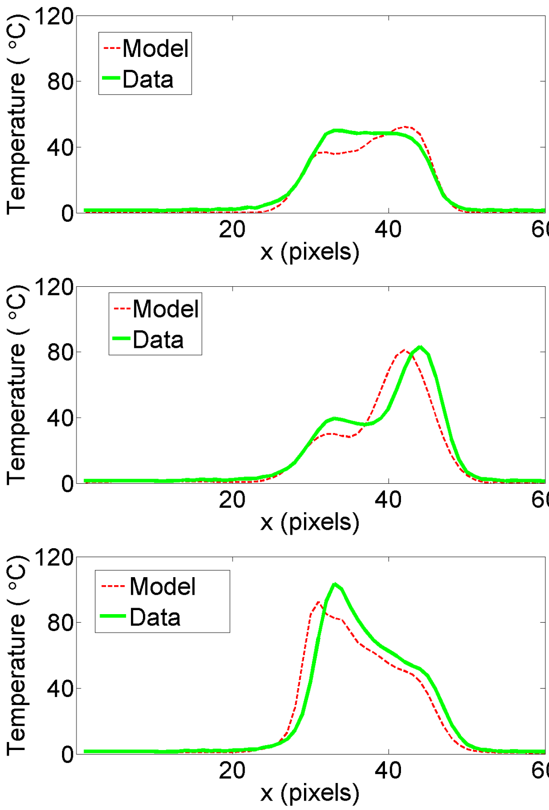

Fig. 9. Validation experiments. Sensor data (solid green line) and the corresponding temperature predicted by the model (dashed red line).

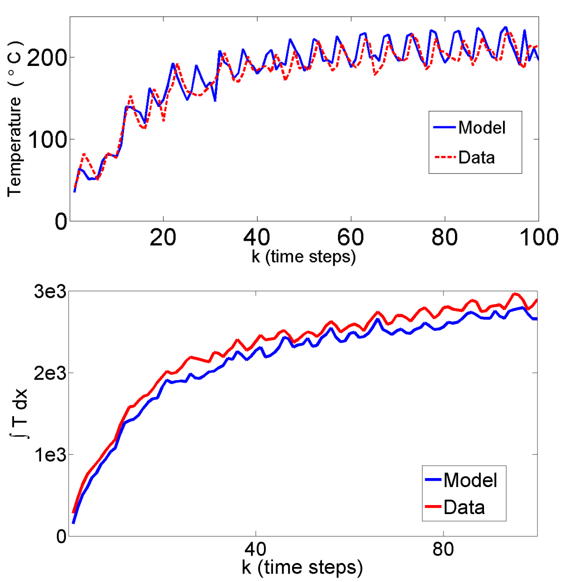

Fig. 10. Validation experiment. Maximum values of temperature for each time step are presented (top). The integral of the area under the curve for each time step is also presented (down).

of living tissue – e.g. blood perfusion – can be neglected to a first approximation [6], additional experiments will be performed to validate the proposed modeling approach for in-vivo applications. Experiments presented in this paper were performed under controlled power conditions (P=3W), additional data is required to model the behavior of different power settings.

The model presented in this paper was implemented in the software system that controls the motion of the laser beam and the exposure time of the laser. Activation and deactivation of the model is synchronized by the system, allowing online estimation of the temperature of the tissue surface. Once the thermal supervision is available, different policies can be used to prevent thermal damage on the tissue. Modification of the scanning frequency or deactivation of the laser exposure can be manipulated by the central system based on the output of the model.

ACKNOWLEDGMENT

The research leading to these results has received funding from the European Union Seventh Framework Programme FP7/2007- 2013 – Challenge 2 – Cognitive Systems, Interaction, Robotics – under grant agreement μRALP ° 288233.

REFERENCES

[1] M. Rubinstein and W. Armstrong, Transoral laser microsurgery for laryngeal cancer: A primer and review of laser dosimetry, Lasers in Medical Science, vol. 26, no. 1, pp. 113124, 2011.
[2] Y.-T. Wong, C. C. Finley, J. F. G. II, and R. A. Buckmire, Novel CO2 Laser Robotic Controller Outperforms Experienced Laser Operators in Tasks of Accuracy and Performance Repeatability, The Laryngoscope, vol. 121, no. 8, pp. 1738–1742, 2011.
[3] H.-W. Tang, H. Van Brussel, J. Vander Sloten, D. Reynaerts, G. De Win, B. Van Cleynenbreugel, and P. R. Koninckx, Evaluation of an Intuitive Writing Interface in Robot-aided Laser Laparoscopic Surgery. Jnl. of Intl. Soc. of Computer Aided Surgery, vol. 11, no. 1, Jan. 2006.
[4] L. Mattos, N. Deshpande, G. Barresi, L. Guastini, and G. Peretti, A novel computerized surgeon–machine interface for robot-assisted laser phonomicrosurgery, The Laryngoscope, 2014.
[5] P. Saccomandi, E. Schena, S. Silvestri, Techniques for temperature monitoring during laser-induced thermotherapy: An overview. International Journal of Hyperthermia 29 (7), 609-619. 2013.
[6] M. Niemz, Laser-Tissue Interactions: Fundamentals and Applications, ser. Biological and Medical Physics Series. Springer, 2007.
[7] B. Cox, Introduction to laser-tissue interactions, October 2013, Lecture Notes - University College of London.
[8] L. Fichera, D. Pardo, and L. Mattos, Modeling tissue temperature dynamics during laser exposure" in Advances in Computational Intelligence - IWANN13, vol. 7903. Springer Berlin Heidelberg, 2013.
[9] O. Svelto, Principles of Lasers, Springer New York Dordrecht Heidelberg London,2010
[10] L. S. Mattos, G. Dagnino, G. Becattini, M. Dellepiane, and D. G. Caldwell, A Virtual Scalpel System for Computer-assisted Laser Microsurgery, in Proc. IEEE/RSJ Intl. Conf. on Intelligent Robots and Systems, (IROS 2011), Sep. 2011, pp. 1359–1365.
[11] D. M. Bates and D. G. Watts, Nonlinear Regression and Its Applications. New York: Wiley, 1988.
[12] J. J. Crochet, S. C. Gnyawali, Y. Chen, E. C. Lemley, L. V. Wang and W. R. Chen, Temperature distribution in selective laser-tissue. Journal of Biomedical Optics 11(3), 2006.
[13] S. C. Gnyawali, C. Surya, Y. Chen, F. Wu, K .E. Bartels, J. P. Wicksted, H. Liu, C. K. Sen, and W. R. Chen. Temperature measurement on tissue surface during laser irradiation, Medical Biological Engineering Computing,46, 2008.
[14] A. Y. Citekaya, and S. S. Seker, Modeling and Simulation of Temperature Distribution in Laser-tissue Interaction. Progress in Electromagnetics Research Symposium - PIERS, 2011.